Electronic Supplementary Material (ESI) for Lab on a Chip

Synthesis of biomimetic oxygen-carrying compartmentalized microparticles using flow lithography

Harry Z. An, Eric R. Safai, H. Burak Eral and Patrick S. Doyle

Supporting Information

A. Effect of Pluronic F-68 On Droplet Coarsening

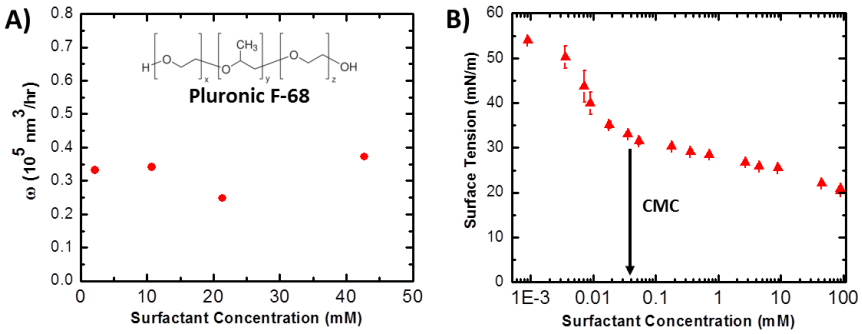

Fig. S1 Variations of (A) Ostwald ripening rate, ω and (B) perfluorodecalin/water surface tension with Pluronic F-68 concentration.

Changing the concentration of Pluronic F-68, a common non-ionic triblock copolymer surfactant (structure shown in Figure S1 inset), has little effect on emulsion stability. To see this, we made 8% by volume perfluorodecalin emulsions containing 36% PEGDA700 at a range of Pluronic F-68 concentrations (~ 2-40 mM) in the continuous phase, and tracked the droplet size over time to extract the corresponding ripening rates. A plot of ω as a function of [PF68] is shown in **Figure S1A**. Within this surfactant concentration regime, which is orders of magnitudes greater than the surfactant's critical micelle concentration (~0.04 mM as determined using the pendant drop method in 1X PBS buffer at room temperature), changes in surface tension, γ, is small, therefore it is not surprising the ripening rate doesn't vary dramatically (see Eq. 1 in the main text).

B. Model Derivation

We use a simple mean-field approach to find the effective diffusivity of oxygen, D, in a dilute oil-in-water emulsion. D captures the O_2 mass transport that occurs on a length scale much greater than the distance between neighboring oil droplets, and allows us to treat a heterogeneous suspension as a homogeneous composite material.

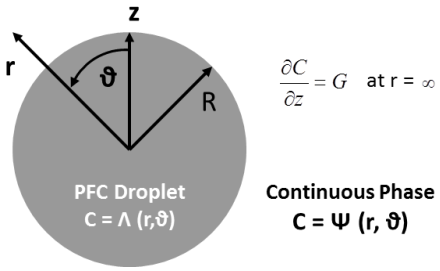

Fig. S2 Model setup. A perfluorocarbon oil droplet of radius R is dispersed in a semi-infinite continuous phase. C denotes the oxygen concentration everywhere in this problem. There is a constant oxygen concentration gradient far from the droplet as a result of the radical polymerization reaction in SFL.

We derive D from the disturbance in the O_2 concentration field far away from an oil droplet. **Figure S1** shows the model geometry: a perfluorocarbon oil droplet is surrounded by an aqueous continuous phase. The oxygen concentration C, is broken down into two distinct regions, separated by the droplet interface.

In spherical coordinates with the origin situated at the center of the droplet, the field variables inside and outside the droplet, respectively, are:

$$\Lambda = f(r,\theta)$$

$$\psi = g(r,\theta)$$

We can write mass conservation equations for O_2 in this system at steady-state, without any volumetric reaction (consumption) terms as:

$$\frac{\partial}{\partial r}\left(r^2\frac{\partial \Lambda}{\partial r}\right)+\frac{1}{\sin\theta}\frac{\partial}{\partial \theta}\left(\sin\theta\frac{\partial \Lambda}{\partial \theta}\right)=0$$

$$\frac{\partial}{\partial r}\left(r^2\frac{\partial \psi}{\partial r}\right)+\frac{1}{\sin\theta}\frac{\partial}{\partial \theta}\left(\sin\theta\frac{\partial \psi}{\partial \theta}\right)=0$$

This set of PDEs captures the diffusive mass transfer after particle gelation has occurred during stop-flow lithography. To expedite the solution procedure, it is easier to make a variable change from θ to η:

$$\eta = \cos\theta$$

η varies from -1 (when θ=180°) to 1 (when θ=0°). The two PDEs above can then be re-written as (Eqs. 9 and 11 in the main text):

$$\frac{\partial}{\partial r}\left(r^2\frac{\partial \Lambda}{\partial r}\right)+\frac{\partial}{\partial \eta}\left((1-\eta^2)\frac{\partial \Lambda}{\partial \eta}\right)=0$$

$$\frac{\partial}{\partial r}\left(r^2\frac{\partial \psi}{\partial r}\right)+\frac{\partial}{\partial \eta}\left((1-\eta^2)\frac{\partial \psi}{\partial \eta}\right)=0$$

Subject to the following four boundary conditions:

At r = R, continuity in O_2 concentration and flux dictates:

$$\Lambda(R,\eta) = K\psi(R,\eta)$$

where K is the partition coefficient; and

$$D_{PFC}\frac{\partial}{\partial r}\Lambda(R,\eta) = D_0\frac{\partial}{\partial r}\psi(R,\eta)$$

Let $\beta = D_{PFC}/D_0$.

At the droplet center (r = 0):

$$\Lambda(0,\eta) = finite$$

And finally, far away from the droplet (r = ∞), there is a constant concentration gradient (due to the polymerization reaction, i.e. bulk consumption of O_2 in the microfluidic device):

$$\frac{\partial}{\partial z}\psi(\infty,\eta) = G$$

Or equivalently, since $z = r\cos\theta = r\,\eta$:

$$\frac{\partial}{\partial r}\psi(\infty,\eta) = G\eta$$

Using the Finite Fourier Transform (FFT) method, and η as the (only) finite dimension, we can transform the governing equations term-by-term using:

$$\Lambda_n = \int_{-1}^{1} \Phi_n(\eta)\Lambda(r,\eta)d\eta$$

$$\psi_n = \int_{-1}^{1} \Phi_n(\eta)\psi(r,\eta)d\eta$$

with $\Phi_n(\eta)$ as the basis functions obtained from Legendre polynomials. Transforming the second-derivative term in r is straightforward, but the term associated with η requires using integration by parts:

$$\int_{-1}^{1} \Phi_n \frac{\partial}{\partial\eta}\left((1-\eta^2)\frac{\partial\Lambda}{\partial\eta}\right)d\eta = (1-\eta^2)(\Phi_n\frac{\partial\Lambda}{\partial\eta} - \Lambda\frac{\partial\Phi_n}{\partial\eta})\Big|_{\eta=-1}^{\eta=1} - n(n+1)\Lambda_n$$

where n = 0, 1, 2... . $n(n+1)$ is the eigenvalues associated with the FFT problem in η.

The transformed governing equations are therefore:

$$\frac{d}{dr}\left(r^2\frac{d\Lambda_n}{dr}\right) - n(n+1)\Lambda_n = 0$$

$$\frac{d}{dr}\left(r^2\frac{d\psi_n}{dr}\right) - n(n+1)\psi_n = 0$$

These are ordinary, second-order differential equations with a generic solution of the form:

$$\Lambda_n = r^m$$

Substituting this into the transformed concentration equation above, we get a quadratic characteristic equation:

$$m^2 + m - n(n+1) = 0$$

which when solved, we obtain:

$$m = n \qquad \text{or} \qquad m = -(n+1)$$

In other words, the general solution for the concentration inside the droplet is:

$$\Lambda_n = A_n r^n + B_n r^{-(n+1)} \qquad \text{n = 0, 1, 2…}$$

where A_n and B_n are series of constants we need to determine using the boundary conditions. Since $[O_2]$ must be finite at the center of the droplet, $B_n = 0$.

Similarly, for the continuous phase:

$$\psi_n = C_n r^n + D_n r^{-(n+1)} \qquad \text{n = 0, 1, 2…}$$

To find A_n, C_n, and D_n, we start by transforming the BC far away at r = ∞,

$$\frac{d}{dr}\psi_n(\infty) = \int_{-1}^{1} \Phi_n(\eta)\frac{\partial}{\partial r}\psi(\infty,\eta)d\eta$$

$$\frac{d}{dr}\psi_n(\infty) = G\int_{-1}^{1} \Phi_n(\eta)\eta d\eta = \sqrt{2/3}\,G\int_{-1}^{1} \Phi_n(\eta)\sqrt{3/2}\,\eta d\eta$$

$$\frac{d}{dr}\psi_n(\infty) = \sqrt{2/3}\,G\delta_{n1}$$

In the last step, we invoked the orthogonality condition (i.e., only the first basis function is required to satisfy the concentration gradient far away). We can analytically express the gradient using the general solution for ψ_n as:

$$\frac{d\psi_n}{dr} = nC_n r^{n-1} - (n+1)D_n r^{-(n+2)}$$

For n = 1 and r =∞ :

$$C_1 = \sqrt{2/3}\,G$$

$C_n = 0$ for all n ≥ 2.

From the BCs at r = R:

$$A_n R^n = K(C_n R^n + D_n R^{-(n+1)})$$

$$\beta\, nA_n R^{n-1} = nC_n R^{n-1} - (n+1)D_n R^{-(n+2)}$$

Solving this set of algebraic equations, we get:

$$A_0 = KC_0$$

$$A_1 = (\frac{3K}{2+\beta})C_1$$

$$D_1 = (\frac{1-\beta}{2+\beta})R^3 C_1$$

All other constants are zero. Assembling the overall concentration profile:

$$C(r,\eta) = \begin{cases} \Lambda(r,\eta) = \dfrac{KC_0}{\sqrt{2}} + \left(\dfrac{3K}{2+\beta}\right)Gr\eta & 0 \le r \le R \\ \psi(r,\eta) = \dfrac{C_0}{\sqrt{2}} + Gr\eta + \left(\dfrac{1-\beta}{2+\beta}\right)\dfrac{R^3}{r^2}G\eta & R < r < \infty \end{cases}$$

Replacing $C_0/\sqrt{2}$ with A, we arrive at Eq. 14 in the main text. C_0 is an arbitrary constant since only a gradient BC is used in this problem. We can see from the expression for ψ, that a PFC droplet of radius R will cause a dipolar disturbance, far away in the O_2 concentration in the surrounding fluid by an amount equal to C_p :

$$C_p(r) = \left(\frac{1-\beta}{2+\beta}\right)\frac{R^3}{r^2}G\eta$$

The total, additive perturbation, then due to a collection of droplets with a number density, n in an arbitrary spherical volume V, of radius a (where a >> R):

$$C_p^{total}(r) = nVR^3\left(\frac{1-\beta}{2+\beta}\right)\frac{G\eta}{r^2} = \varphi a^3\left(\frac{1-\beta}{2+\beta}\right)\frac{G\eta}{r^2}$$

where $\varphi = n\,{}^{4\pi}/_{3}\,R^3$ is the oil volume fraction.

Finally, to derive an expression for D, we compare the equation above with the analogous result obtained by assuming that V is occupied by a homogenous composite material, characterized by diffusivity parameter β'. According to the equation for C_p, a homogenous sphere of radius a will perturb the O_2 concentration in the surrounding fluid by:

$$C_p^{total}(r) = \left(\frac{1-\beta'}{2+\beta'}\right)\frac{a^3}{r^2}G\eta$$

We equate the two equations for C_p^{total} and solve for β':

$$\left(\frac{1-\beta'}{2+\beta'}\right) = \varphi\left(\frac{1-\beta}{2+\beta}\right)$$

Let B = $\left(\frac{1-\beta}{2+\beta}\right)$,

$$1-\beta' = \varphi B(2+\beta') = 2\varphi B + \varphi B\beta'$$

$$\beta' = \frac{-2\varphi B + 1}{\varphi B + 1}$$

Using Taylor expansion in φ, for a dilute emulsion:

$$\beta' = \frac{D}{D_0} = 1 - 3B\,\varphi + O(\varphi^2) = 1 - 3\left(\frac{1-\beta}{2+\beta}\right)\varphi + O(\varphi^2)$$

Slight rearrangement and ignoring higher order terms, yields Eq. 16 in the main text.

$$D = D_0\left(1 + 3\left(\frac{\beta-1}{\beta+2}\right)\varphi\right)$$

The key results to an analogous problem related to the effective conductivity of a particle suspension have been presented in Deen [1]. The full solution is included for reference.

C. Dilution Effects on Droplet Coalescence

For composite particle synthesis, it is highly desirable to be able to arbitrarily tune the volume fraction of the encapsulated oil droplets. However, for the PFC system, it is important to maintain the surfactant concentration in the bulk throughout the dilution process. To see this, we diluted an 8.5% PFC nanoemulsion stock (C_s=20 mM, P=0.36 PEGDA700) down to 0.2% using pure continuous phase (P=0.36 PEGDA700) with (**Figure S3** upper-left) and without surfactant (lower-left). The droplets were labeled with 10 μM PKH26 for fluorescence microscopy. In the case of the latter, droplets underwent coalescence presumably related the dynamics of the surfactant repartitioning between the droplet interface and the bulk as more diluent was introduced.

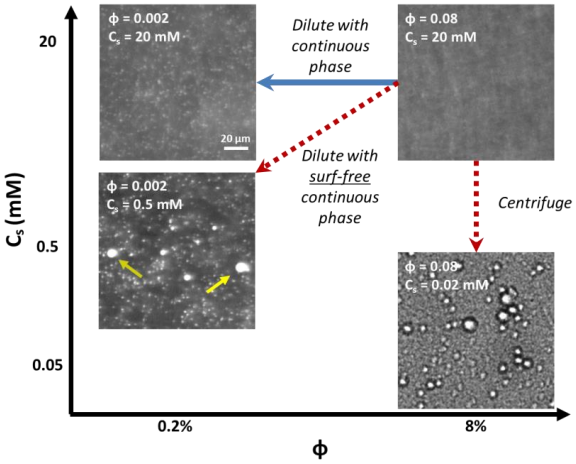

Fig. S3 Phase diagram. Fluorescent and bright-field (lower-right corner) micrographs showing droplet coalescence caused by dilution of a concentrated nanoemulsion stock (ϕ_1=0.08, ϕ_2=0.005, C_s=20 mM).

As mentioned in the main text, packaging nanoemulsion droplets in gel particles provides a convenient route to arbitrarily lower the bulk surfactant concentration (**Figure 7**). It is worth noting that we could not reduce the concentration of PF68 by ultracentrifuging and decanting a concentrated (8.5%) emulsion stock directly without causing droplet coalescence (**Figure S3**, lower-right).

D. Particle Shape Anisotropy

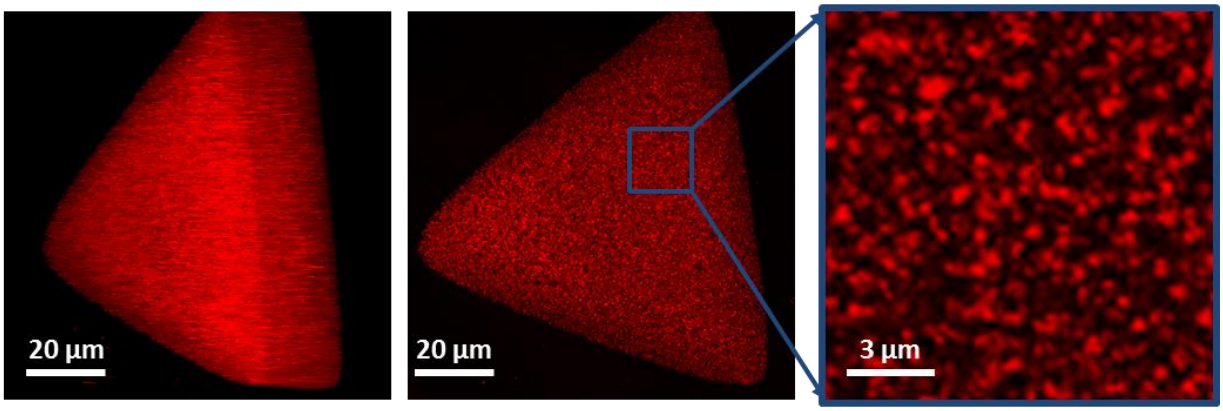

Fig. S4 Confocal micrograph of a large triangle-shaped particles (100 µm/side, φ_1=0.08, φ_2=0.005, C=20 mM , P=0.36 PEGDA, PI = 0.04) synthesized using SFL. The average diameter of the encapsulated droplets is ~200 nm.

Modifying the setup for SFL doesn't impede with our ability to tune the particle morphology. Indeed, we can make any 2D-extruded shapes using this projection-based lithography technique by inserting photomasks with the desirable particle cross-sectional geometry prior to synthesis. As an example, representative confocal images of a large triangle-shaped particle are shown in **Figure S4**. The droplets, which are pre-labeled with 10 µM PKH26, are homogeneously distributed throughout the particle.

E. Droplet Aggregation

We note that more direct methods of expediting polymerization kinetics, such as increasing the crosslinker (PEGDA700) concentration in the continuous phase, or raising the photoinitiator concentration (beyond ~4% by volume), both resulted in droplet aggregation, which could be due to depletion type forces (**Figure S5A, B**). Once the droplet flocs formed (labeled using PKH26), we could no longer make microparticles with homogenous loading (**Figure S5C**).

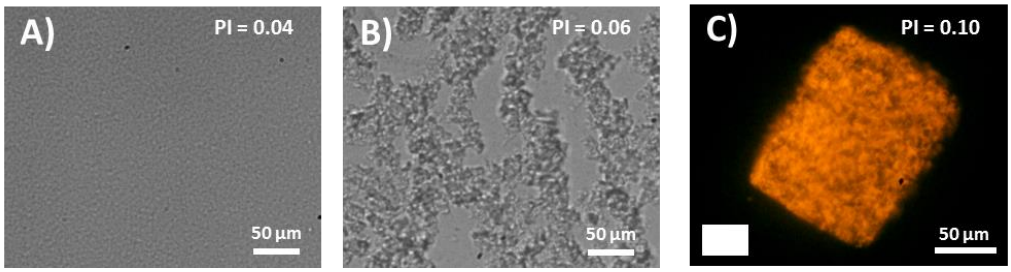

Fig. S5 Droplet aggregation. Micrographs of a 8.5% by volume PFC nanoemulsion (φ_1=0.08, φ_2=0.005, C=20 mM , P=0.36 PEGDA) of (A) 4% photoinitiator, (B) 6% photoinitiator, and (C) 10% photoinitiator made into a rectangle-shaped particle using SFL.

F. Estimating the Encapsulated Oil Volume Fraction From Confocal Images

From stacks of *z* scans taken via confocal microscopy, we first identified particles using visual inspection in ImageJ. We manually selected every bright spot in each slice. If a spot appeared in 4 to 5 slices consecutively (Δz = 0.1 µm), we considered it as a single droplet.

To estimate the encapsulated volume fraction, we needed three pieces of information: 1) the droplet count in a single slice (measured as previously discussed), 2) the average droplet diameter in the prepolymer solution (measured using DLS), and 3) the imaging volume within the composite particle (diameter, $2R_h$~20 µm). The latter was calculated as the product of the in-plane area multiplied by the effective focal depth. The effective focal depth was calculated by summing the focal depth of the microscope (d_f) and the size of two droplets ($4\langle R\rangle$). The droplet size needed to be taken into account since some droplets contributing to the overall droplet count could be adjacent to the imaging volume as illustrated in **Figure S6**. In a typical slice, we found ~20 droplets. The focal depth for the imaging conditions used in our experiments was ~0.8 µm. The droplets appeared to be ~0.4 µm due to a combination of the point-spread function under fluorescence mode and finite exposure time. Substituting the quantities in, the encapsulated volume fraction equals $20 * \frac{4\pi*(0.2)^3}{3} / (1.6 * \pi * 10^2)$ =1.2x10^{-4}. The error in assessing the encapsulated volume fraction can be estimated using the following equation, which takes into account droplet polydispersity ($\frac{d\langle R\rangle}{\langle R\rangle}$~0.2) and resolution of the microscope (in measuring the dimensions of the gel particles, dR_h~100 nm):

$$\frac{d\varphi}{\varphi} = \sqrt{3\left(\frac{d\langle R\rangle}{\langle R\rangle}\right)^2 + 2\left(\frac{dR_h}{R_h}\right)^2}$$

Substituting values, we get $\frac{d\varphi}{\varphi}$~0.34 or 34%. The difference of 20% we found is within this error bound.

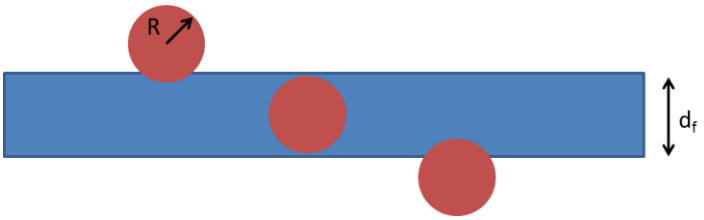

Figure S6 Illustration of the effective focal depth.

G. Estimating the oxygen-carrying ability of a 10 µm x 10 µm composite particle

We estimated the maximum amount of oxygen that a 10µm (diameter) by 10µm (height) PFC nanoemulsion compsite particle can hold by measuring the oxygen solubility of the prepolymer constituents (i.e., 36% PEGDA in water, perfluorodecalin). We assumed that the oxygen solubilities of perfluorodecalin and perfluorotripropylamine are the same. The oxygen concentration measurements were performed *in-situ*, non-invasively using the RedEye oxygen sensing patches (FOXY, Ocean Optics). This

technique is based on the dynamic, and reversible, phosphorescence quenching of an indicator dye by oxygen. The degree of quenching correlates with the partial pressure of oxygen in the RedEye patch (a sol-gel matrix with embeded dye). During an experiment, a specially engineerd bifurcated optical fiber (RE-BIFBORO-2) is pointed at the RedEye patch. The fiber produces directs a blue LED excitation light toward the patch, and excites the O_2-sensitive sensor dye. The red emitted signal is then collected by the optical probe and transmitted to a fluorometer, which measures the phosphorescence lifetime, τ. τ is related to the partial pressure of oxygen by the well-known Stern-Volmer Equation [2]. Lifetime-based O_2 detection is a more robust, and quantitative alternative to traditional intensity-based detection methods, which are prone to photodegradation.

To estimate the oxygen-carrying ability of the PFC-composite microgels, we performed oxygen sensing experiments in 36% PEGDA in water (7.7 ppm) and perfluorodecalin (95 ppm). Prior to each measurement, we calibrated the RedEye probe using a recommended 2-point calibration procedure (at 0% O_2 and 20.9% O_2) at room temperature. Given the particle dimensions (10 μm diameter and 10 μm height) and composition (8.5% perfluorocarbon oils), we estimated the maximum amount of oxygen it is able to hold by using a volume-average expression (Eq. 6).

$$[O_2] = 0.915(7.7ppm) + 0.085(95ppm) = 15.1 \text{ mg/L}$$

On a per particle basis, the mass of O_2 amounts to ~10^{-11} mg. In comparison to a purely PEG-based particle of the same size (i.e., no oil droplets of any kind), the PFC composite can carry *~100% more oxygen*. This is in good agreement with our assumptions made in the main text.

1. Deen, W.M., *Analysis of Transport Phenomena.* 1998.
2. Papkovsky, D.B. and R.I. Dmitriev, *Biological detection by optical oxygen sensing.* Chemical Society Reviews, 2013.